



Sensitivity analysis of operating parameters of proton exchange membrane fuel cells

Fei Liu^{1,2,3} · Xichao Li^{1,2,3} · Peiwen Zhao^{1,2,3} · Xianwei Sun^{1,2,3} · Jingxiang Zhao^{1,2,3} · Jun Shen⁴ · Zuoqiang Dai^{1,2,3} · Lili Zheng^{1,2,3}

Received: 6 June 2023 / Revised: 10 August 2023 / Accepted: 23 August 2023 / Published online: 25 September 2023
© The Author(s), under exclusive licence to Springer-Verlag GmbH Germany, part of Springer Nature 2023

Abstract

The sensitivity of the operating parameters of proton exchange membrane fuel cells is essential to improve the performance and water management capabilities of the stack. The current research on proton exchange membrane fuel cell sensitivity is mainly focused on simulations and experimental methods for small activation area single cells, but less research literature for commercial stack with larger effective area. In this work, a commercial stack with an effective area of 300 cm² membrane electrode is as the research object. The polarization curves under different operating conditions are obtained by experiment, and the voltage data are processed with first-order derivatives to systematically analyze the effects of gas relative humidity, stoichiometric ratio, inlet gas pressure and operating temperature on the performance of the stack. It was found that a certain degree of cathode inlet relative humidity, cathode stoichiometry ratio, inlet pressure and temperature are beneficial to the stack performance and are closely related to stack water management. However, with the cathode gas relative humidity reaching 45%, the cathode stoichiometry ratio increasing to 1.9 and the operating temperature increasing to 76°C, the stack performance does not improve significantly. And the excessive increase in operating parameters is likely to have a negative impact on the stack performance. The stack performance is less sensitive to the anode stoichiometry ratio and anode gas relative humidity, and when the anode stoichiometry ratio is lower than 1.3, it will have a great negative impact on the stack performance. These are important for the development of controlling the operating parameters for commercial fuel cell.

Keywords Fuel cells · Relative humidity · Stoichiometric ratio · Intake pressure · Operating temperature · Sensitivity

Introduction

The natural attribute of hydrogen energy is clean and low carbon, and under the dual carbon goal, hydrogen energy will create a new and huge industrial ecosystem [1–3]. From the national policy to the material component companies, all of them are making unremitting efforts for the application of hydrogen energy [4, 5]. The proton exchange membrane fuel cell (PEMFC) is a promising energy conversion device with the advantages of high power density, fast dynamic response and no pollution, which plays an important role in the development of new energy vehicles and hydrogen energy applications [6, 7].

Depending on the power requirements of the vehicle, hundreds of single cells are required to be stacked together to form a power stack. The performance, energy conversion efficiency and life of the stack are closely related to the operating parameters such as intake humidity, intake flow, pressure and temperature [8–11]. Zhao et al. [12] measured

✉ Zuoqiang Dai
daizuoqiangqdu@163.com

✉ Lili Zheng
llzhengqdu@163.com

¹ College of Mechanical and Electrical Engineering, Qingdao University, Qingdao 266071, China

² Engineering Technology Center of Power Integration and Energy Storage System, Qingdao University, Qingdao 266071, China

³ National and Local Joint Engineering Technology Center for Intelligent Power Integration Technology of Electric Vehicles (Qingdao), Qingdao 266071, China

⁴ Hydra Power (Qingdao) Energy Technology Co., Ltd, Qingdao 266100, China

the humidity under different conditions by embedding a cathodic flow field microsensor and combining with electrochemical impedance spectroscopy to show that the relative humidity has a significant effect on the internal resistance of the PEMFC. Humidification of the inlet gas can effectively mitigate the low relative humidity and membrane dewatering caused by excessive temperature. At the same time, the high humidity gas makes the water management downstream of the flow field face a severe test. Miao et al. [13] found that increasing the relative humidity was effective in improving membrane hydration in the inlet region; however, at high current densities, high relative humidity led to local flooding in the outlet region. Wang et al. [14] investigated the effect of operating parameters on PEMFC performance and durability under hydrogen-deficient conditions using a segmentation technique. The results showed that the durability of the PEMFC is closely related to the relative humidity and that high relative humidity at the inlet leads to severe carbon corrosion. Hasheminasab et al. [15] investigated the effect of temperature and stoichiometric ratio on water management and performance of parallel serpentine flow channels. It was found that an increase in the inlet gas temperature led to a decrease in the accumulated liquid water content of the flow channel and improved performance due to enhanced reaction kinetics. At the same time, the increase in stoichiometry led to a decrease in the accumulated water content of the flow channel, resulting in membrane dehydration, which also facilitated the entry of reactants into the reaction site. Zhang et al. [16] used electrochemical impedance spectroscopy to analyze the sensitivity of a single cell with an effective area of 25 cm^2 to operating parameters. The cell temperature, pressure, stoichiometric ratio and inlet relative humidity had a large effect on the impedance spectrum. Wang et al. [17] studied the distribution of liquid water and temperature under different operating conditions and physical parameters by developing a three-dimensional non-isothermal two-phase flow model. Kahveci et al. [18] investigated the effect of operating parameters on PEMFC performance by developing a three-dimensional single-phase model. It was found that the PEMFC performance increased with increasing operating pressure. Meanwhile, temperature has an important effect on the performance of PEMFC, and the cell performance decreases when a certain temperature is exceeded. Rizvandi et al. [19] investigated the effect of operating conditions on cell performance in the anode leakage mode by building simulations. Wang et al. [20] investigated the effects of operating parameters such as cathode relative humidity, stoichiometric ratio and inlet pressure on the performance of PEMFC anode recirculation by dynamic simulation. The PEMFC membrane water content is closely related to the transport mechanism of water in the membrane, while the inlet pressure, operating temperature and pressure difference have important effects on

the transport of water and protons in the membrane. Wang et al. [21] investigated the diffusion mechanism of hydrated hydrogen ions and water molecules under pressure difference by a nonequilibrium molecular dynamics model. The results showed that the proton conductivity increased with the pressure difference, and the transport diffusion coefficients of water molecules and hydrated hydrogen ions were positively correlated with temperature. Similarly, Trinh et al. [22] designed an experimental configuration to investigate the diffusion mechanism of water through the membrane and demonstrated that the membrane water content and diffusion coefficient were proportional to the operating temperature.

Researchers have conducted numerous studies on the sensitivity of fuel cells with small activation areas through simulations and experiments, but there is less research literature on stacks with larger effective areas [23–27]. Therefore, the effective area of 300 cm^2 fuel cell was studied experimentally. Through quantitative comparison and analysis of stack performance, the influence of stack temperature, intake humidity, pressure and stoichiometry ratio on its performance was studied. At the same time, an in-depth analysis of its influence mechanism and causes has important reference significance for stack performance optimization.

Experimental

Experimental conditions

In this study, a stack of four single cells with an effective area of 300 cm^2 is used. The bipolar plate (BP) is graphite material, and the flow field is parallel flow channel. The membrane electrode assembly (MEA) produced by a domestic manufacturer was used, with Pt loading of 0.27 mg cm^{-2} and 0.05 mg cm^{-2} for the cathode and anode catalyst layers, respectively, and the thickness of the gas diffusion layer was 0.145 mm . The proton exchange membrane was Gore M820.15, and the carbon paper was produced by Toray. As shown in Fig. 1, the air intake is forced convection. Figure 2 shows a 2kW test stand manufactured by Qunyi Energy Co.

Operating parameter sensitivity experiments

PEMFC is activated by gas humidification and variable current activation program for about 3 h. The maximum current density of the experiment is 1600 mA cm^{-2} . Short-term activation is performed at the end of each experiment, trying to ensure that the initial state of each experiment is consistent. The stack operating parameters are shown in Table 1 to study the effects of stack operating temperature, inlet humidity, pressure and stoichiometric ratio on its performance at different current densities. Here, the coolant inlet temperature is used to define the operating temperature of the stack. Run for 5 min at each

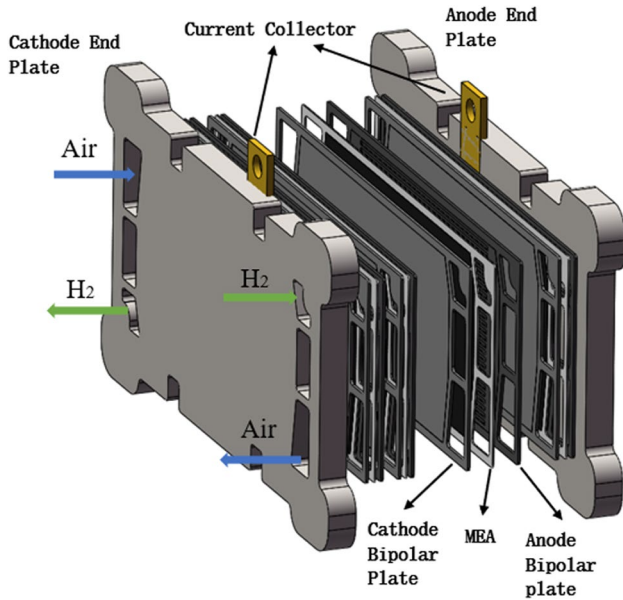


Fig. 1 Schematic diagram of stack assembly



Fig. 2 Experimental system setup

current density to reach steady state and record the PEMFC polarization curves for different operating conditions.

Sensitivity analysis methods

The fuel cell performance is the result of coupling multiple factors of input and output, and the output voltage can be expressed by the following formula.

$$V = f(RH, ST, P, T) \tag{1}$$

where *RH* is humidity, *ST* is stoichiometric ratio, *P* is gas pressure and *T* is stack temperature. In this paper, the sensitivity of operating parameters is analyzed by the rate of change of voltage. It is expressed by the following equation.

$$R_i = \frac{f(RH + \Delta, ST, P, T) - f(RH, ST, P, T)}{\Delta} \times 100\% \tag{2}$$

where Δ is the value of the humidity change, and the numerator indicates the voltage difference corresponding to the humidity change.

Results and analysis

Humidity sensitivity analysis

The generation of water in the proton exchange membrane fuel cell occurs mainly on the cathode side, and the sources of water on the anode side of the stack can be divided into gas humidification, concentration diffusion, electric drag, pressure migration and water carried by hydrogen recirculation [28–30].

The ionic conductivity is highly dependent on the water content of the membrane, which increases as the membrane water content increases. The ionic conductivity of proton exchange membrane can be expressed by the following equation [31].

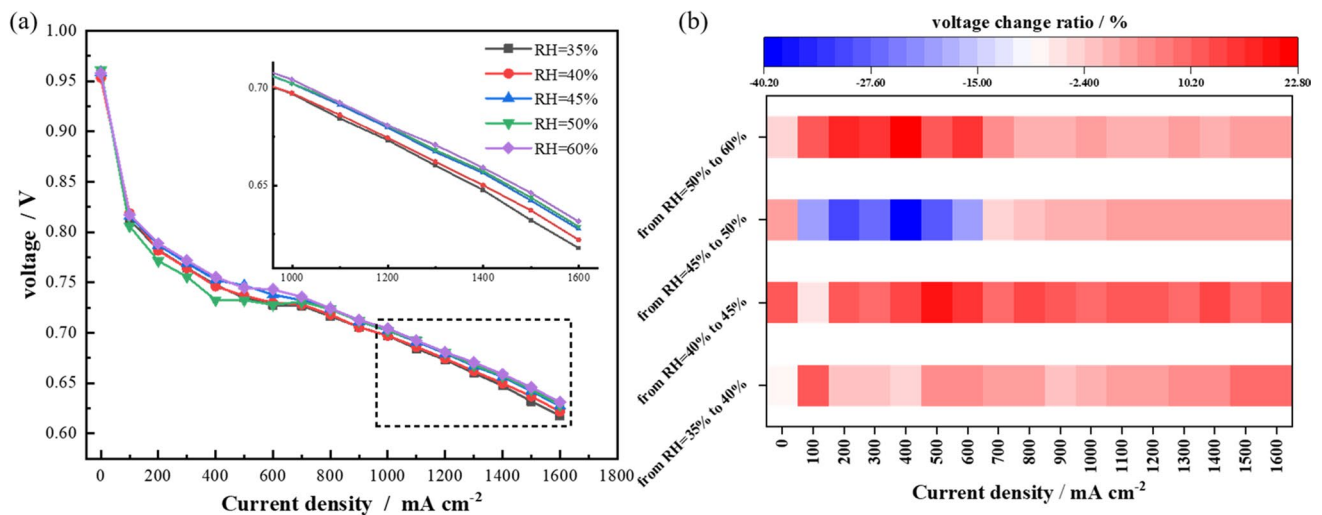
$$\kappa_{ion} = (0.5139\lambda - 0.326) \exp\left(1268\left(\frac{1}{303.15} - \frac{1}{T}\right)\right) \tag{3}$$

λ is the membrane water content, and *T* is the stack operating temperature.

Figure 3 shows the stack polarization curves and voltage change rates for 35 to 60% relative humidity of the cathode, corresponding to Cases 1 and Case 6–9. In the low current density region, the performance is rather better at lower inlet RH of 35%, 40%, and 45% relative to the cathode inlet RH of 50%, while the high-frequency resistance (HFR) is maximum at 50% RH (Fig. 4). This may be due to the different initial state of the membrane after the pre-test running and shelving, making the lower inlet humidity test result an improvement in performance instead. This also makes the voltage fluctuate more from 45 to 50% relative humidity and from 50 to 60% relative humidity (Fig. 3b). The test results excluding the 50% relative humidity condition clearly yielded that as the inlet relative humidity increased, its voltage at the same current density increased, and the performance is positively correlated with the inlet relative humidity (Fig. 3a). Moreover, as the relative humidity increases, it makes the

Table 1 Experimental operating conditions

Case number	Anode stoichiometric ratio	Cathodic stoichiometric ratio	Anode inlet gas pressure (kPag)	Cathode inlet gas pressure (kPag)	Anode relative humidity	Cathode relative humidity	Operating temperature (°C)
Case 1	1.6	2	140	120	40%	50%	75
Case 2	1.6	2	140	120	50%	50%	75
Case 3	1.6	2	140	120	60%	50%	75
Case 4	1.6	2	140	120	70%	50%	75
Case 5	1.6	2	140	120	80%	50%	75
Case 6	1.6	2	140	120	40%	35%	75
Case 7	1.6	2	140	120	40%	40%	75
Case 8	1.6	2	140	120	40%	45%	75
Case 9	1.6	2	140	120	40%	60%	75
Case 10	1.6	1.6	140	120	40%	50%	75
Case 11	1.6	1.7	140	120	40%	50%	75
Case 12	1.6	1.8	140	120	40%	50%	75
Case 13	1.6	1.9	140	120	40%	50%	75
Case 14	1.2	2	140	120	40%	50%	75
Case 15	1.3	2	140	120	40%	50%	75
Case 16	1.4	2	140	120	40%	50%	75
Case 17	1.5	2	140	120	40%	50%	75
Case 18	1.6	2	130	110	40%	50%	75
Case 19	1.6	2	135	115	40%	50%	75
Case 20	1.6	2	145	125	40%	50%	75
Case 21	1.6	2	150	130	40%	50%	75
Case 22	1.6	2	140	120	40%	50%	64
Case 23	1.6	2	140	120	40%	50%	68
Case 24	1.6	2	140	120	40%	50%	72
Case 25	1.6	2	140	120	40%	50%	76
Case 26	1.6	2	140	120	40%	50%	78
Case 27	1.6	2	140	120	40%	50%	80

**Fig. 3** **a** Cathodic humidity sensitivity polarization curve; **b** voltage change rate

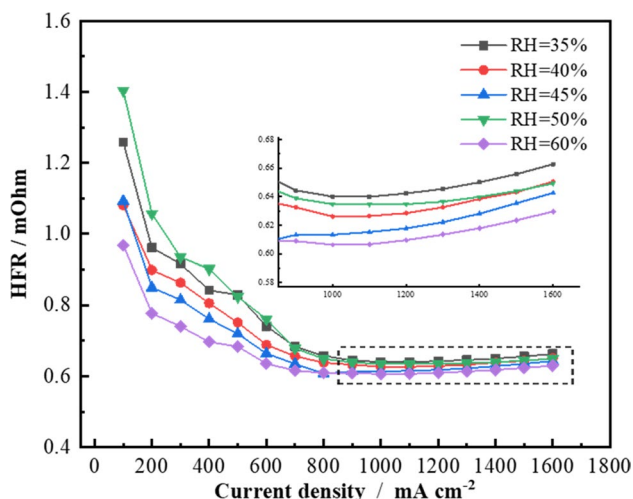


Fig. 4 Cathodic humidity sensitivity HFR

HFR decrease, which facilitates the wetting of the membrane (Fig. 4). From Fig. 3b, it can be seen that in the high current density region, the voltage variation rate is small between the relative humidity from 45 to 50% and the relative humidity from 50 to 60%. The performance improvement is limited as the relative humidity increases, and the cathode-side back-end drainage faces a severe test if the relative humidity is too large. In the low current density region, there is a significant increase in voltage from 40 to 45% and from 50 to 60% relative humidity. The performance of the stack is more sensitive to the inlet relative humidity in the low-density region than in the high-density region. Therefore, the relative humidity tends to stabilize at around 50%, and the relative humidity is best in the 50 to 60% region.

Figure 5a shows the stack polarization curves for the anode relative humidity interval from 40 to 80%, corresponding to Cases 1–5. In the low current density region, the voltage fluctuation is large and irregular in the 500–800 mA cm⁻² region, which is caused by the poor membrane hydration state and the initial state consistency problem of the stack. In the high current density region, the voltage increases with increasing anode inlet humidity, except for the low voltage at 70% relative humidity. In the overall analysis, the increase of anode relative humidity has a positive effect on the stack performance. As evident from the rate of voltage change in Figs. 3b and 5b, the anode inlet relative humidity sensitivity is lower, and the performance improvement is limited compared to the cathode side. At a current density of 1600 mA cm⁻², the voltage change rate of the cathode gas relative humidity from 35 to 60% is 5.46%, while the voltage change rate of the anode gas relative humidity from 40 to 80% is only 0.96%. This is due to the lower gas flow rate on the anode side, and the water carried off by the gas is much smaller than that on the cathode side. Also, liquid water driven by capillary pressure is the main source of water in the membrane on the anode side [32]. Therefore, the effect of anode gas relative humidity on the stack performance will be greatly reduced.

Stoichiometric ratio sensitivity analysis

In the low current density region, larger stoichiometric ratios are usually used to ensure the concentration of reactants inside the reactor and to avoid the single-low phenomenon of single-cell voltage due to low reactant concentration. In the high current density region, the reaction produces more water which is more likely to cause flooding of the stack, and

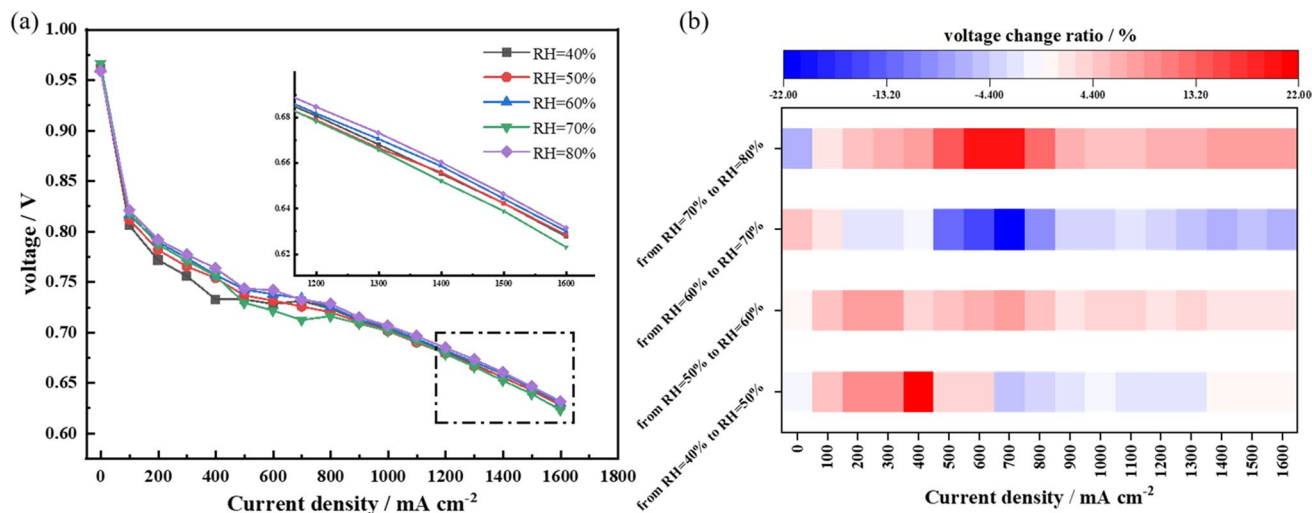


Fig. 5 a Anode humidity sensitivity polarization curve; b voltage change rate

the stoichiometric ratio has a greater impact on its performance. Therefore, stoichiometric ratio sensitivity studies in the high current density region are the main focus.

Figures 6 and 7 show the polarization curves, the rate of voltage change and HFR for cathode stoichiometry ratios from 1.6 to 2.0, corresponding to Cases 1 and Case 10–13. As the cathode stoichiometry ratio increases, the voltage increases in the high current density region (Fig. 6). It is obvious from Fig. 6b that the stoichiometric ratio is from 1.8 to 1.9 region, the rate of voltage change is larger and there is a significant improvement in performance. And as the current density increases, the more obvious the effect on the performance. While in the stoichiometric ratio from 1.9 to 2.0 region, the rate of voltage change is small, and there is no significant change in performance. With the increase of stoichiometric ratio, the inlet gas volume and airflow velocity increase, which can avoid the rapid decrease of reactant concentration caused by electrochemical reaction and enhance the mass transfer capability. As the gas flow rate increases, the pressure drop becomes larger, resulting in a lower partial pressure of water vapor, which subsequently leads to a lower relative humidity of the gas at the outlet and carries away a large amount of water [32]. As shown in Fig. 7, as the cathode stoichiometry ratio increases, the HFR increases and the membrane water content decreases. Too large stoichiometric ratios can cause slight dehydration of the membrane. At the same time, the membrane water content on the inlet side is lower, and the consistency within the membrane is worse, which also has an impact on the lifetime of the stack. Cathode stoichiometry ratios above 2 may cause a decrease in performance, and the increased energy consumption from increasing the stoichiometry ratio should also be considered. Therefore, an optimum value of cathode

stoichiometry ratio exists in the interval of 1.9 to 2.0, which makes the best performance of the stack.

The gas flow rate on the anode side is smaller compared to the cathode side. Therefore, the increase in the anode stoichiometry ratio, compared to the cathode side, is less for the pressure drop inside the stack and less water is carried off by the gas. At the same time, there is enough liquid water transfer from the cathode side to the anode side to ensure the stability of the membrane water content. From the anode stoichiometry sensitivity data in Fig. 8, it is clear that the voltage variation rate is only 0.93% in the anode stoichiometry ratio 1.3–1.6 interval at 1600 mA cm⁻² current density. From the polarization curves in Fig. 8a and the voltage change rate in Fig. 8b, it is obvious that in the anode stoichiometry ratio 1.2–1.3 interval, the voltage change rate is 12.35% with the decrease of stoichiometry ratio, which has a significant decrease. At the same time, the single cell voltage appears single low phenomenon, which is caused by the lack of hydrogen in the partial area, and this phenomenon may become more obvious with the increase of the single cell of the stack. In the operation of the stack, the gas concentration inside the stack should be ensured while improving the energy utilization. Therefore, the anode stoichiometry ratio should not be lower than 1.3.

Pressure sensitivity analysis

In the pressure sensitivity test, the inlet pressure is controlled. A fixed pressure difference of 20 kPa is used for the cathode and anode. Combined with the actual stack system output, in the low current density region, the same inlet pressure is used in the case, and the inlet pressure increases with increasing current density. After the current density was increased to 800 mA cm⁻², a fixed inlet pressure is

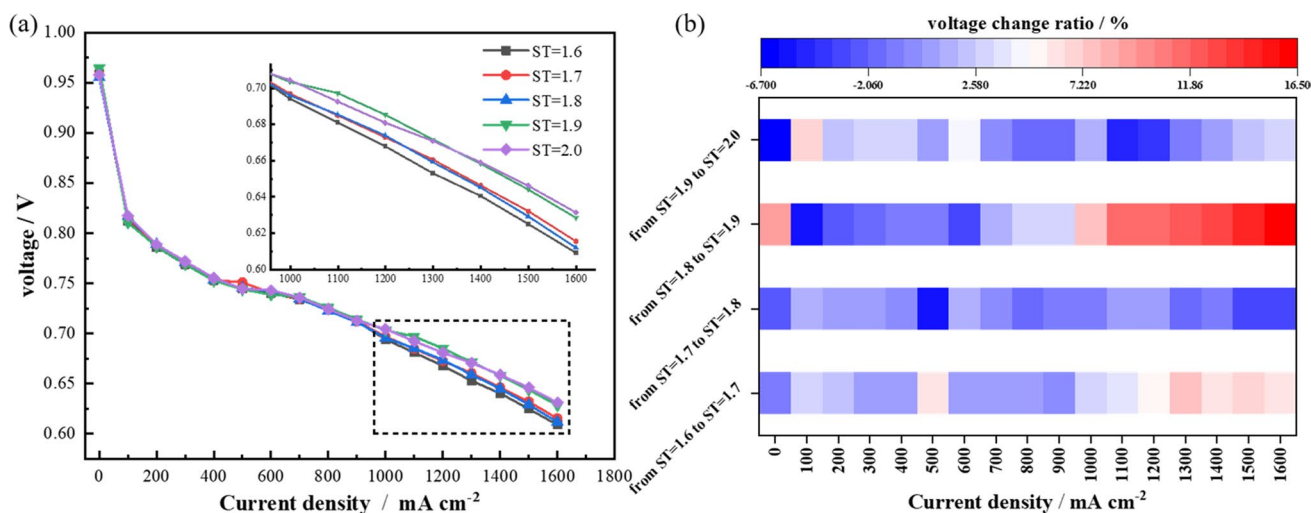


Fig. 6 **a** Cathode stoichiometric ratio sensitive polarization curve; **b** voltage exchange rate

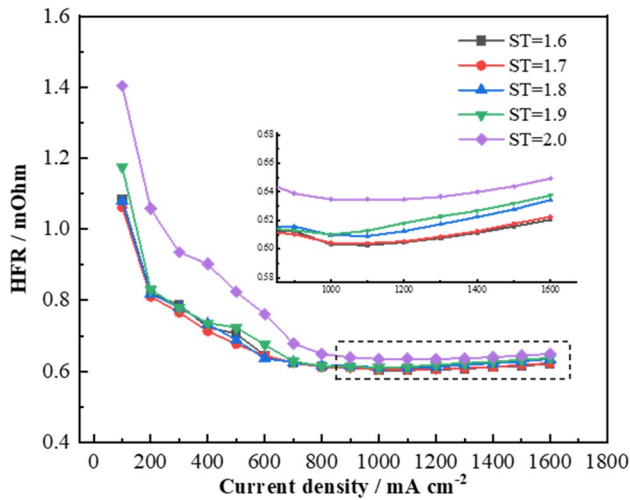


Fig. 7 Cathode stoichiometry ratio sensitivity HFR

adopted. The anode inlet pressure was gradually increased from 130 to 150 kPag for inlet pressure sensitivity testing, with specific parameters corresponding to cases 1 and case 18–21 in Table 1.

From Fig. 9a, it can be seen that after the current density of 800 mA cm^{-2} , the voltage increases to different degrees with the increase of gas pressure. In the high current density region, the rate of voltage change tends to increase as the current density increases (Fig. 9b). It can be seen that the effect of gas pressure on the performance of the stack increases with the increase of current density. This is due to the increase of the concentration polarization with the increase of the current density. And the increase of the working pressure of the stack is beneficial to improve the mass transfer capacity and reduce

the internal resistance. The gas pressure also affects the partial pressure of water vapor inside the PEMFC. It is difficult for water vapor to reach the saturation state at low inlet relative humidity and high stack temperatures. The relative humidity is the actual water vapor pressure and the ratio of saturation to water vapor pressure; saturation vapor pressure is only related to the temperature, and then increasing the pressure makes the water vapor more likely to reach the saturation state, which in turn is conducive to membrane hydration. At a constant cathodic stoic., the mass flow rate of air will not change at elevated pressures. But the gas flow rate will be reduced; thus, less product water is able to evaporate, counteracting drying out of the membranes. Some experiments show that for every 50 kPa increase in PEMFC pressure, the relative humidity will increase by 10~20% [12]. From the test results, it is clear that increasing the inlet pressure is beneficial to the performance of the stack. However, in practical applications, the damage to the membrane caused by excessive operating pressure and the power consumption due to excessive inlet pressure should be avoided. In the high current density region, the pressure operation parameters are refined according to the degree of pressure impact on performance and the balance of auxiliary device power consumption to make the stack operate at the optimal output power state.

Temperature sensitivity analysis

During the temperature sensitivity test, the temperature is fixed at a current density of 100 mA cm^{-2} to 1600 mA cm^{-2} , corresponding to cases 22–27. The coolant inlet temperature is used to indicate the stack temperature, while in actual operation, the stack temperature is higher than the coolant temperature.

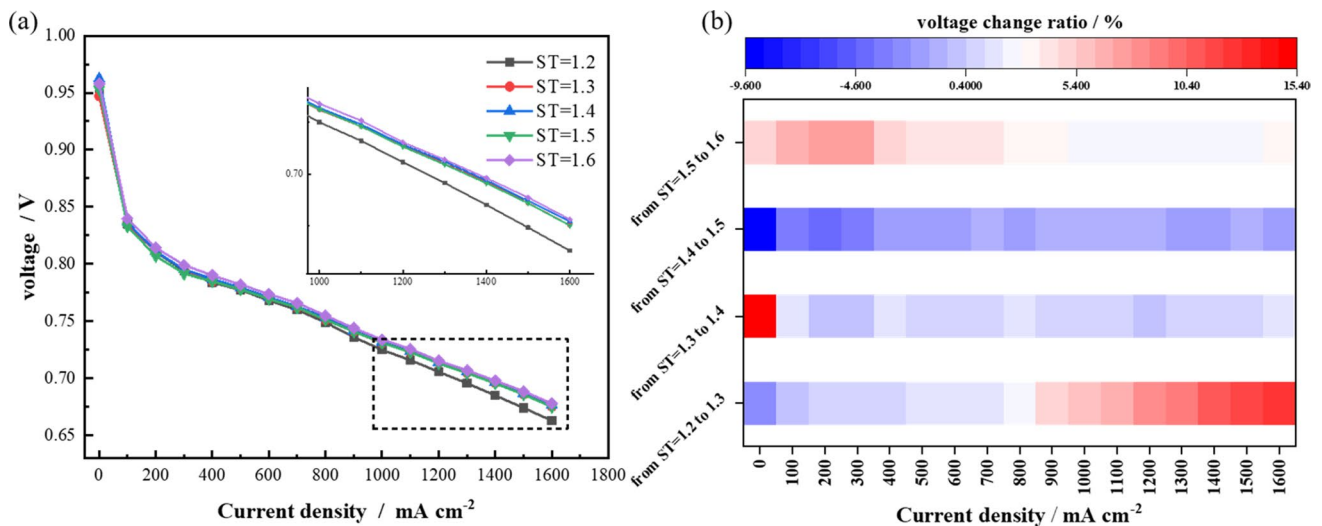


Fig. 8 a Anode stoichiometry ratio sensitive polarization curve; b voltage change rate

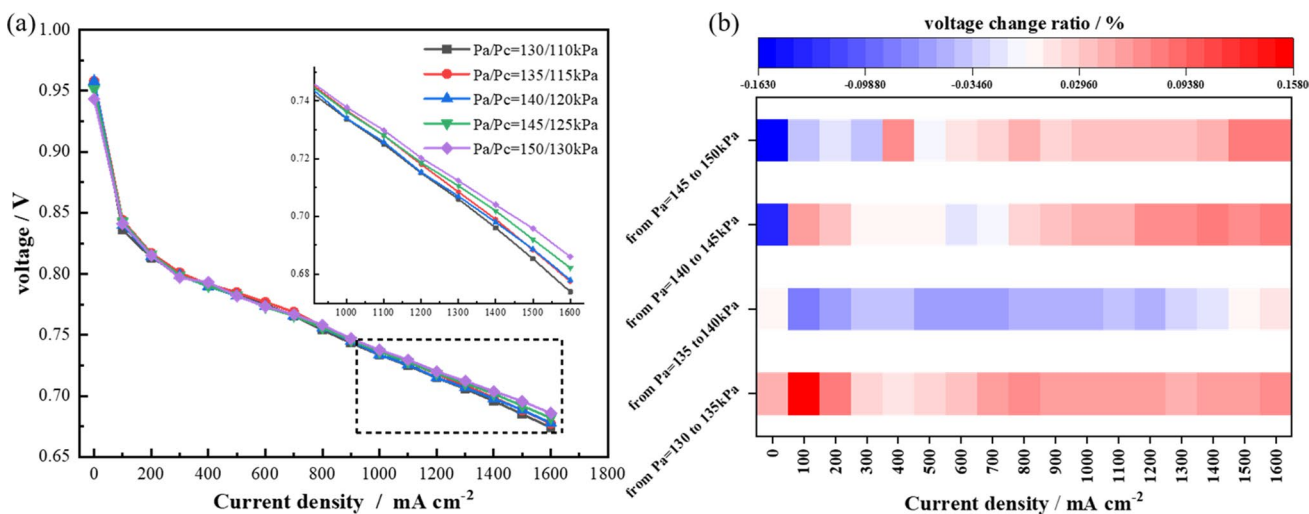


Fig. 9 a Inlet pressure-sensitive polarization curve; b voltage change rate

The operating temperature of the stack is closely related to the saturated vapor pressure, and the saturated vapor pressure P_{sat} and temperature T can be expressed by the following formula [33, 34].

$$\log_{10} \frac{P_{sat}}{101325} = -2.1794 + 0.02953(T - 273.15) - 9.1837 \times 10^{-5}(T - 273.15)^2 + 1.4454 \times 10^{-7}(T - 273.15)^3 \quad (4)$$

P_{sat} is positively correlated with T , and the saturation vapor pressure increases from 23.9 to 47.3 kPa as the temperature increases from 64 to 80°C. Relative humidity is defined as the ratio of the partial pressure of water vapor to the saturated water vapor pressure. It can be seen that a gas with a fixed flow rate can hold more water as the temperature of the gas increases. Thus, as the relative humidity decreases, the water

in the membrane is more easily carried away by the gas. Some studies have shown that the relationship between membrane saturation water content and temperature is more complex, with membrane saturation water content tending to increase at the beginning and then decreasing with increasing temperature [35, 36]. This indicates that there is a limit to the maximum saturated water content of the membrane, and reducing the membrane water content will reduce the ionic conductivity. From Eq. (3), it can be seen that the ionic conductivity increases with the increase in temperature at a constant membrane water content. Therefore, it can be inferred that there is a critical state that makes the ionic conductivity maximum.

In the low current density region, the voltage decreases instead as the temperature of the stack increases (Fig. 10). This is due to the fact that in the low current density

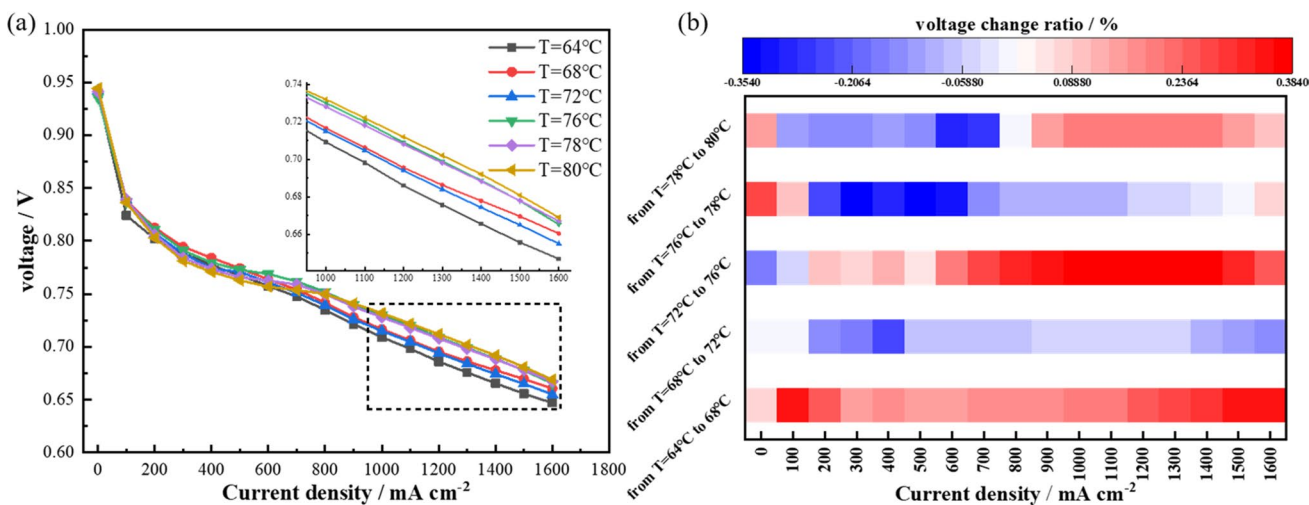


Fig. 10 a Inlet temperature-sensitive polarization curve; b voltage change rate

region, less water is produced by the stack reaction, while the increase in temperature makes the water more easily carried off by the gas, causing an increase in the internal resistance of the membrane. In the high current density region, the stack voltage increases significantly as the temperature increases to 80°C. In particular, there is a significant increase in voltage from a temperature of 72 to 76°C (Fig. 10b). This is due to the fact that in a certain temperature range, as the temperature increases, it facilitates the electrochemical reaction and also improves the electrical conductivity and reduces the ohmic polarization loss. And the large amount of water is produced by the reaction in the high current density region, which can completely offset the more water carried off by the gas due to the increase in temperature. It can also be seen from Fig. 10b that the performance enhancement rate slows down after the temperature is greater than 76°C. Therefore, it can be inferred that as the temperature exceeds 80°C, it is highly likely that the relative humidity of the gas cannot meet the humidification conditions of the stack, and the membrane becomes dehydrated leading to performance degradation.

Conclusions

In this study, for the membrane electrode with larger effective area, the polarization curves under different operating conditions are obtained experimentally, and the data are reprocessed to systematically analyze the effects of gas relative humidity, stoichiometric ratio, inlet pressure and operating temperature on the performance of the stack. The following conclusions can be drawn.

(1) The increase in gas relative humidity contributes to membrane hydration. For the cathode side, there is a significant improvement in the stack performance with the increase of gas relative humidity. However, as the relative humidity increases from 45 to 60%, the stack performance improvement is smaller. Compared to the cathode side, the anode side is less sensitive to the gas relative humidity, and the voltage improvement is limited with the change of the gas humidity.

(2) The performance in the high current density region improved significantly with the increase of cathode stoichiometry ratio. The performance improvement is limited when the cathode stoichiometry ratio increases to 1.9. Excessive stoichiometry ratios may cause dehydration of the membrane and performance degradation. The anode is less sensitive to stoichiometric ratio, but the stoichiometric ratio should not be lower than 1.3; otherwise, there will be significant performance degradation.

(3) Relative humidity increases with increasing inlet pressure, which is favorable for membrane hydration. Also,

the effect of inlet pressure on the performance of the stack increases with the increase of current density.

(4) In the low current density region, the amount of water produced by the stack reaction is less, and the higher operating temperature causes more water to be removed, resulting in reduced performance. In the high current density region, as the temperature increases, the electrochemical reaction is enhanced, and the stack performance is improved. And the performance improvement is smaller after the temperature of the stack exceeds 76°C. Too high temperatures can lead to performance degradation due to dehydration of the membrane as the gas relative humidity does not meet the humidification conditions of the stack.

Author contribution FL: formal analysis, methodology, data curation, writing—original draft, writing—review and editing. XL: investigation, resources, formal analysis. PZ: conceptualization, methodology, software. XS: investigation, resources. JZ: validation, formal analysis. JS: visualization, writing—review and editing. ZD: conceptualization, investigation, supervision, writing—review and editing. LZ: supervision, writing—review and editing.

Data availability Data will be made available on request to the corresponding author.

Declarations

Ethical approval Not applicable.

Competing interests The authors declare no competing interests.

References

1. Fan LX, Tu ZK, Chan SH (2023) Recent development in design a state-of-art proton exchange membrane fuel cell from stack to system: theory, integration and prospective. *Int J Hydrog Energy* 48:7828–7865. <https://doi.org/10.1016/j.ijhydene.2022.11.212>
2. Eicke L, De Blasio N (2022) Green hydrogen value chains in the industrial sector-geopolitical and market implications. *Energy Res Soc Sci* 93:11. <https://doi.org/10.1016/j.erss.2022.102847>
3. Yang Y, Tong LG, Yin SW et al (2022) Status and challenges of applications and industry chain technologies of hydrogen in the context of carbon neutrality. *J Clean Prod* 376:26. <https://doi.org/10.1016/j.jclepro.2022.134347>
4. Kong F, Wang YF (2022) How to understand carbon neutrality in the context of climate change? With special reference to China COMMENT. *Environ. Sustain.* 8:1–14. <https://doi.org/10.1080/27658511.2022.2062824>
5. Zou CN, Li JM, Zhang X et al (2022) Industrial status, technological progress, challenges, and prospects of hydrogen energy. *Nat. Gas Ind. B.* 9:427–447. <https://doi.org/10.1016/j.ngib.2022.04.0062352-8540>
6. Luo Y, Wu YH, Li B et al (2021) Development and application of fuel cells in the automobile industry. *J. Energy Storage* 42:19. <https://doi.org/10.1016/j.est.2021.103124>
7. Olabi AG, Wilberforce T, Abdelkareem MA (2021) Fuel cell application in the automotive industry and future perspective. *Energy* 214:18. <https://doi.org/10.1016/j.energy.2020.118955>

8. Li YH, Pei PC, Wu ZY et al (2018) Approaches to avoid flooding in association with pressure drop in proton exchange membrane fuel cells. *Appl Energy* 224:42–51. <https://doi.org/10.1016/j.apenergy.2018.04.071>
9. Kim YS, Kim DK, Ahn KY et al (2020) Real-time analysis of dry start-up characteristics of polymer electrolyte membrane fuel cell with water storage process under pressurized condition. *Energy* 199:8. <https://doi.org/10.1016/j.energy.2020.117292>
10. Kravos A, Ritzberger D, Hametner C et al (2021) Methodology for efficient parametrisation of electrochemical PEMFC model for virtual observers: model based optimal design of experiments supported by parameter sensitivity analysis. *Int J Hydrog Energy* 46:13832–13844. <https://doi.org/10.1016/j.ijhydene.2020.10.146>
11. Yang L, Chen T, Liu S et al (2019) Effect of temperature and back pressure on the performance of PEMFC. *Battery Bimonthly* 49:364–367. <https://doi.org/10.19535/j.1001-1579.2019.05.001>
12. Zhao JJ, Tu ZK, Chan SH (2022) In-situ measurement of humidity distribution and its effect on the performance of a proton exchange membrane fuel cell. *Energy* 239:13. <https://doi.org/10.1016/j.energy.2021.122270>
13. Miao TW, Tongsh CS, Wang JN et al (2022) Current density and temperature distribution measurement and homogeneity analysis for a large-area proton exchange membrane fuel cell. *Energy* 239:12. <https://doi.org/10.1016/j.energy.2021.121922>
14. Wang YJ, Xie XJ, Zhou C et al (2020) Study of relative humidity on durability of the reversal tolerant proton exchange membrane fuel cell anode using a segmented cell. *J Power Sources* 449:9. <https://doi.org/10.1016/j.jpowsour.2019.227542>
15. Hasheminasab M, Kermani MJ, Nourazar SS et al (2020) A novel experimental based statistical study for water management in proton exchange membrane fuel cells. *Appl Energy* 264:16. <https://doi.org/10.1016/j.apenergy.2020.114713>
16. Zhang S, Dai H, Yuan H et al (2021) Sensibility study on electrochemical impedance of proton exchange membrane fuel cell. *J. Mech. Eng.* 57:40–51. <https://doi.org/10.3901/JME.2021.14.040>
17. Wang ZM, Xu C, Wang XY et al (2021) Numerical investigation of water and temperature distributions in a proton exchange membrane electrolysis cell. *Sci. China Technol. Sci.* 64:1555–1566. <https://doi.org/10.1007/s11431-021-1810-9>
18. Kahveci EE, Taymaz I (2018) Assessment of single-serpentine PEM fuel cell model developed by computational fluid dynamics. *Fuel* 217:51–58. <https://doi.org/10.1016/j.fuel.2017.12.073>
19. Rizvandi OB, Eskin MG, Yesilyurt S (2021) Numerical modeling of anode-bleeding PEM fuel cells: effects of operating conditions and flow field design. *Int J Hydrog Energy* 46:4378–4398. <https://doi.org/10.1016/j.ijhydene.2020.10.228>
20. Wang BW, Wu KC, Xi FQ et al (2019) Numerical analysis of operating conditions effects on PEMFC with anode recirculation. *Energy* 173:844–856. <https://doi.org/10.1016/j.energy.2019.02.115>
21. Wang G, Liu Z, Liu C et al (2023) Molecular study of nonequilibrium transport mechanism for proton and water in porous proton exchange membranes. *Int J Energy Res* 2023:13. <https://doi.org/10.1155/2023/1138198>
22. Trinh NV, Nguyen XL, Kim Y et al (2022) Characteristics of water transport of membrane electrolyte over selected temperature for proton exchange membrane fuel cell. *Polymers* 14:13. <https://doi.org/10.3390/polym14152972>
23. Jiang Y, Yang ZR, Jiao K et al (2018) Sensitivity analysis of uncertain parameters based on an improved proton exchange membrane fuel cell analytical model. *Energy Convers Manag* 164:639–654. <https://doi.org/10.1016/j.enconman.2018.03.002>
24. Gong ZC, Wang BW, Wu KC et al (2022) A 1+1-D multiphase proton exchange membrane fuel cell model for real-time simulation. *IEEE Trans. Transp. Electrification* 8:2928–2944. <https://doi.org/10.1109/tte.2021.3115794>
25. Yang ZR, Du Q, Jia ZW et al (2019) A comprehensive proton exchange membrane fuel cell system model integrating various auxiliary subsystems. *Appl Energy* 256:18. <https://doi.org/10.1016/j.apenergy.2019.113959>
26. Yang Z, Li Y, Ji X et al (2022) Sensitivity analysis of operating parameters for proton exchange membrane fuel cells. *J Jilin Univ Eng Technol Edition* 52:1971–1981. <https://doi.org/10.13229/j.cnki.jdxbgxb20220355>
27. Xia G, Zhang X, Ma D et al (2022) Parameter sensitivity analysis of proton exchange membrane fuel cell. *Acta Energetica Sinica* 43:493–499. <https://doi.org/10.19912/j.0254-0096.tynxb.2022-0238>
28. Dickinson EJJ, Smith G (2020) Modelling the proton-conductive membrane in practical polymer electrolyte membrane fuel cell (PEMFC) simulation: a review. *Membranes* 10:53. <https://doi.org/10.3390/membranes10110310>
29. Futter GA, Gazdzicki P, Friedrich A et al (2018) Physical modeling of polymer-electrolyte membrane fuel cells: understanding water management and impedance spectra. *J Power Sources* 391:148–161. <https://doi.org/10.1016/j.jpowsour.2018.04.070>
30. Chen L, Chen YY, Tao WQ (2023) Schroeder's paradox in proton exchange membrane fuel cells: a review. *Renew Sustain Energy Rev* 173:23. <https://doi.org/10.1016/j.rser.2022.113050>
31. Zhang Y, He SR, Jiang XH et al (2023) Three-dimensional simulation of large-scale proton exchange membrane fuel cell considering the liquid water removal characteristics on the cathode side. *Int J Hydrog Energy* 48:10160–10179. <https://doi.org/10.1016/j.ijhydene.2022.11.343>
32. Kim DK, Choi EJ, Song HH et al (2016) Experimental and numerical study on the water transport behavior through Nafion (R) 117 for polymer electrolyte membrane fuel cell. *J Membr Sci* 497:194–208. <https://doi.org/10.1016/j.memsci.2015.09.053>
33. Huo S, Li LC, Shi WY et al (2021) Characteristics of cold start behavior of PEM fuel cell with metal foam as cathode flow field under subfreezing temperature. *Int. J. Green Energy* 18:1129–1146. <https://doi.org/10.1080/15435075.2021.1891911>
34. Chen L, Chen YY, Tao WQ (2023) Schroeders paradox in proton exchange membrane fuel cells: a review. *Renew Sustain Energy Rev* 173:23. <https://doi.org/10.1016/j.rser.2022.113050>
35. Maldonado L, Perrin JC, Dillet J et al (2012) Characterization of polymer electrolyte Nafion membranes: influence of temperature, heat treatment and drying protocol on sorption and transport properties. *J Membr Sci* 389:43–56. <https://doi.org/10.1016/j.memsci.2011.10.014>
36. Li QF, He RH, Jensen JO et al (2003) Approaches and recent development of polymer electrolyte membranes for fuel cells operating above 100 degrees C. *Chem Mater* 15:4896–4915. <https://doi.org/10.1021/cm0310519>

Publisher's Note Springer Nature remains neutral with regard to jurisdictional claims in published maps and institutional affiliations.

Springer Nature or its licensor (e.g. a society or other partner) holds exclusive rights to this article under a publishing agreement with the author(s) or other rightsholder(s); author self-archiving of the accepted manuscript version of this article is solely governed by the terms of such publishing agreement and applicable law.